2013 10th International Conference on Ubiquitous Robots and Ambient Intelligence (URAI)
October 31-November 2, 2013 / Ramada Plaza Jeju Hotel, Jeju, Korea

Swarm control of cell-based microrobots using a single global magnetic field

Paul Seung Soo Kim[1], Aaron Becker[2], and Yan Ou[3], Anak Agung Julius[3], Min Jun Kim[1]
[1] Department of Mechanical Engineering and Mechanics, Drexel University, Philadelphia, PA 19104, USA
(Tel : +1-215-895-2295; E-mail: psk25@drexel.edu, mkim@coe.drexel.edu)
[2] Computer Science Department, Rice University, Houston, TX 77005, USA
(Tel : +1-713-348-4539; E-mail: aaron.becker@rice.edu)
[3] Department of Electrical, Computer, and Systems Engineering, Rensselaer Polytechnic Institute, Troy, NY 12180, USA
(Tel : +1-518-276-6993; E-mail: ouy2@rpi.edu, agung@rpi.edu)

Abstract – *Tetrahymena pyriformis* is a single cell eukaryote that can be modified to respond to magnetic fields, a response called magnetotaxis. In experiments, a rotating field is applied to cells using a two dimensional approximate Helmholtz system. Using rotating magnetic fields, we characterize discrete cells' swarm swimming which is affected by several factors. The behavior of the cells under these fields is explained in detail. After the field is removed, relatively straight swimming is observed. By exploiting this straight swimming behavior, we propose a method to control discrete cells utilizing a single global input. Successful implementation of this swarm control method would enable teams of microrobots to perform a variety of microscale tasks impossible for single microrobots, such as pushing objects or simultaneous micromanipulation of discrete entities.

Keywords – *Tetrahymena pyriformis*, magnetotaxis, swarm control, microrobot

1. Introduction

Navigating microrobots through low Reynolds number fluids is a large hurdle of robotics. In low Reynolds number environments, viscous forces dominate over inertial forces, and traditional methods of swimming will not work. Nature has developed methods to overcome viscous forces, such as cilia and flagella, through the use of non-reciprocal motion. Many research groups have looked to nature for inspiration and have developed such robotic microswimmers [1-10]. While these robots are capable of swimming in microfluidic environments, they are not able to be controlled to discrete points. We have developed a versatile microrobot platform: we focus on the well-studied [11] protozoan *Tetrahymena pyriformis* (*T. pyriformis*). This microorganism makes a capable robot, as it has sensing abilities (sensory organelles), a powerful propulsion system (cilia that propels the cell up to 1000 μm/s, or 20× its body length), is powered by its environment (takes nutrients in from its surroundings), and is cheap to produce in mass (cell culturing), making it an ideal candidate for a microrobot.

To control microorganisms, specifically *T. pyriformis*, their behavioral response to stimuli is utilized. This response is known as a taxis. *T. pyriformis* has exhibited galvanotaxis (response to electric fields) [12-14], chemotaxis (chemical gradient) [15, 16], and phototaxis (light) [14]. While abiotic microrobot platforms exploit the specificity of engineered inorganic actuators, it is a great obstacle to imbed onboard sensing equipment analogous to the sensory organelles found in microorganisms. As a result, we are greatly interested in further characterizing *T. pyriformis* as a microrobot and organic actuator.

Magnetic fields are a great tool to control objects in the respect that they are able to be implemented globally without affecting other materials. Magnetic fields have been used by researchers to control bacteria [17-19] as well as abiotic microswimmers [3, 5]. By having *T. pyriformis* ingest iron oxide particles, the cells can be steered using magnetic fields after the magnetite is magnetized. The global nature of magnetic fields makes discrete control difficult. Nevertheless, using a three-dimensional approximate Helmholtz system, a single *T. pyriformis* has been controlled and tracked in three dimensions [20]. Feedback algorithms and computer controlled magnetic fields have also been used to steer the cells [21, 22].

Artificially magnetotactic *T. pyriformis* (AMT) align under a uniform magnetic field due to the torque generated. The response and time to align itself to a magnetic field is partially a function of the magnetic dipole strength, which is different for all cells. By exploiting the various responsiveness of the cells to magnetic fields, multiple cells may be able to be controlled using a single global magnetic field. In this paper, we explore the swimming behavior of AMT under rotating magnetic fields in detail, and propose a method for controlling a swarm of cells based on the results.

2. Materials and Methods

2.1 *Tetrahymena pyriformis* culturing

T. pyriformis (Fig. 1, left) is cultured in a standard growth medium composed of 0.1% w/v select yeast extract (Sigma Aldrich, St. Louis, MO) and 1% w/v tryptone (Sigma Aldrich, St. Louis, MO) in deionized water. Cell lines are maintained by transferring a small amount of

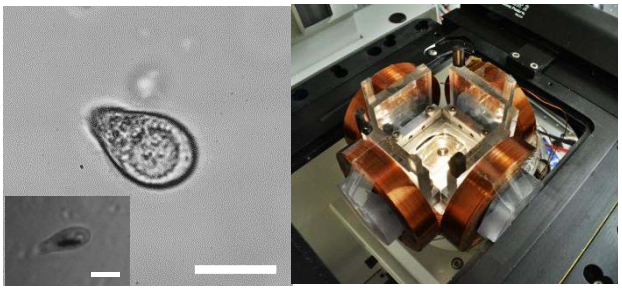

Fig. 1. (left) A single *Tetrahymena pyriformis* cell without any ingested iron oxide. (inset) A cell with internatlized magnetized iron oxide. The scale bar ares 25 µm. (right) Two pairs of approximate Helmholtz coils integrated into a microscope stage.

cells into fresh medium weekly and incubated at 28 °C. Cells typically reach full saturation in 48 hours [23]. *T. pyriformis* is a pear shaped cell that is 25 µm × 50 µm in size. It is a powerful swimmer, resulting from the arrays of ~600 cilia on its body. The cell utilizes two types of cilia: oral (for ingesting particles) and motile (arranged in arrays along the cells length used for swimming). The ciliary arrays on the cell are on a slight axis, resulting in a corkscrew motion during swimming

2.2 Artificially Magnetotactic *T. pyriformis*

T. pyriformis normally does not normally respond to magnetic fields, but we have developed a method to make them artificially magnetotactic. 50 nm iron oxide particles (Sigma Aldrich, St. Louis, MO) are added to culture medium with *T. pyriformis* and then gently agitated to ensure uptake of the magnetite. The cells ingest these particles through their oral apparatus and enclose them in vesicles. The solution of cells is exposed to a permanent neodymium-iron-boron magnet (K&J Magnetics, Pipersville, PA) with a surface field strength of 1964 gauss. This magnetizes the ingested iron oxide, as the particles should be fully saturated to react with the applied rotational magnetic fields. This exposure also separates the cells from the extraneous particles not consumed in the solution. After magnetization, the ingested iron oxide forms a rod like shape inside the cell body along the cell's major axis due to the N-S poles. When a magnetic field is applied, the torque generated can be calculated using,

$$\tau = \boldsymbol{m} \times \boldsymbol{B} = mB \sin\theta \qquad (1)$$

where τ, $\boldsymbol{m}$, and $\boldsymbol{B}$ represent the torque, magnetic moment, and the magnetic field, respectively. θ is the angle difference between the magnetic moment and the magnetic field. If the cell is orientated in a direction such that there is some nonzero value of θ, a torque will be generated, steering the cell to the direction of the magnetic field. Thus, when the cell is aligned with a magnetic field, no torque is generated and the cell will continue to swim along this magnetic field.

Artificially magnetotactic *T. pyriformis* (AMT) exhibit axial magnetotaxis. When cells are exposed to a permanent magnet after ingesting iron oxide, the

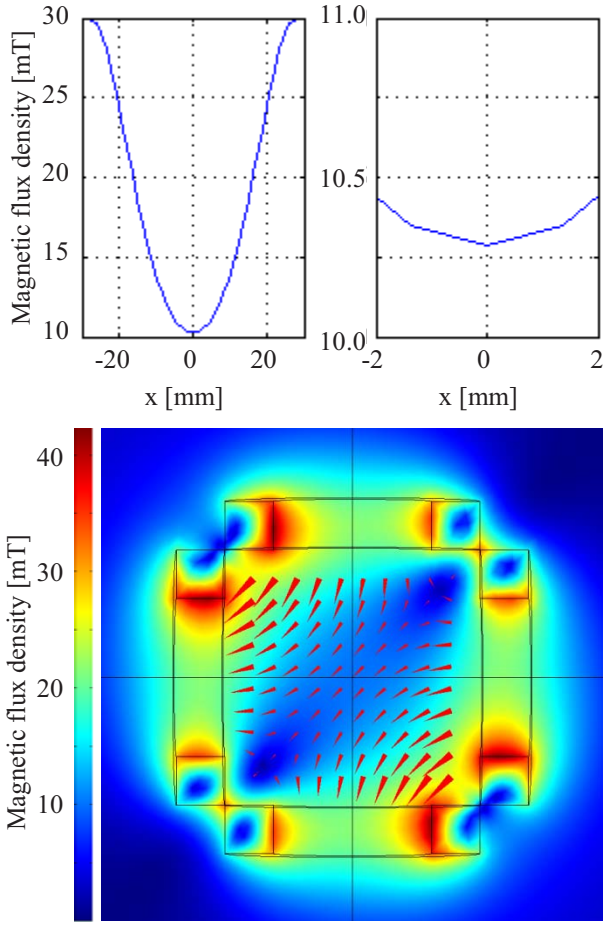

Fig. 2. Simulation of magnetic field strength of our 2D approximate Helmholtz coil system. (top) There is a negligible magnetic field gradient across an area of 2 mm, approximately the same size as the field of view of our experiments. These plots represents the field strength for both the *x* and *y*-axes. The uniformity of this field indicates that translation due to a magnetic field gradient is negligible. (bottom) The direction of the magnetic fields are indicated by the red vectors. The area between the coils is 6.25 mm × 6.25 mm.

internalized iron oxide becomes magnetized. However, the orientation of the dipole is random. That is, some cells will have a north to south polarity from the cell anterior to posterior, while other cells have the polarity reversed. This results in cells aligning themselves to any applied magnetic field, but they may swim in opposite directions. In experiments where a rotating magnetic field was implemented, the orientation of swimming AMT may differ in phase by ~180°. Experiments were conducted within an hour after magnetization, during which we assume the dipole strength remains constant.

2.3 Experimental Setup

Cells are placed in an 80 µm deep microchannel to minimize any fluid flow and for ease of visualization. Microchannels are fabricated using SU-8 molds on silicon wafers made using standard photolithography techniques

[24]. An elastomer and curing agent mixture is poured onto silanized SU-8 molds. The resulting cured PDMS mold is then adhered onto glass slides using oxygen plasma treatment. Microchannels containing AMT are placed on the stage of an inverted LEICA DM IRB microscope. Images are captured with a Photron Fastcam SA3 using a 4× objective at 125 frames per second. An Edmund Optics 3112C CMOS camera is used to image cells with a 10× objective at 21.49 frames per second.

At the center of the microscope stage is an approximate 2D Helmholtz coil system. Two pairs of electromagnetics are placed on the x and y-axes to generate uniform magnetic field in 2 dimensions. Microchannels are placed on the center of the system, as shown in Fig. 1 (right). Because the magnetic field gradient (Fig. 2) is negligible, we assumed there is no translation force from any non-uniform gradient and that only a torque is generated. LabVIEW is used to generate a constant rotational input at 6 rad/s through two power supplies (one for each axis). The position and orientation of cells are calculated using an image processing algorithm in MATLAB. Because of the axial magnetotactic nature of the cells, cells aligned on a magnetic field moving in opposite directions have a phase difference of 180°. The orientation of cells have been modified so all cells aligned to the magnetic field will have a θ value of 0 for better evaluation.

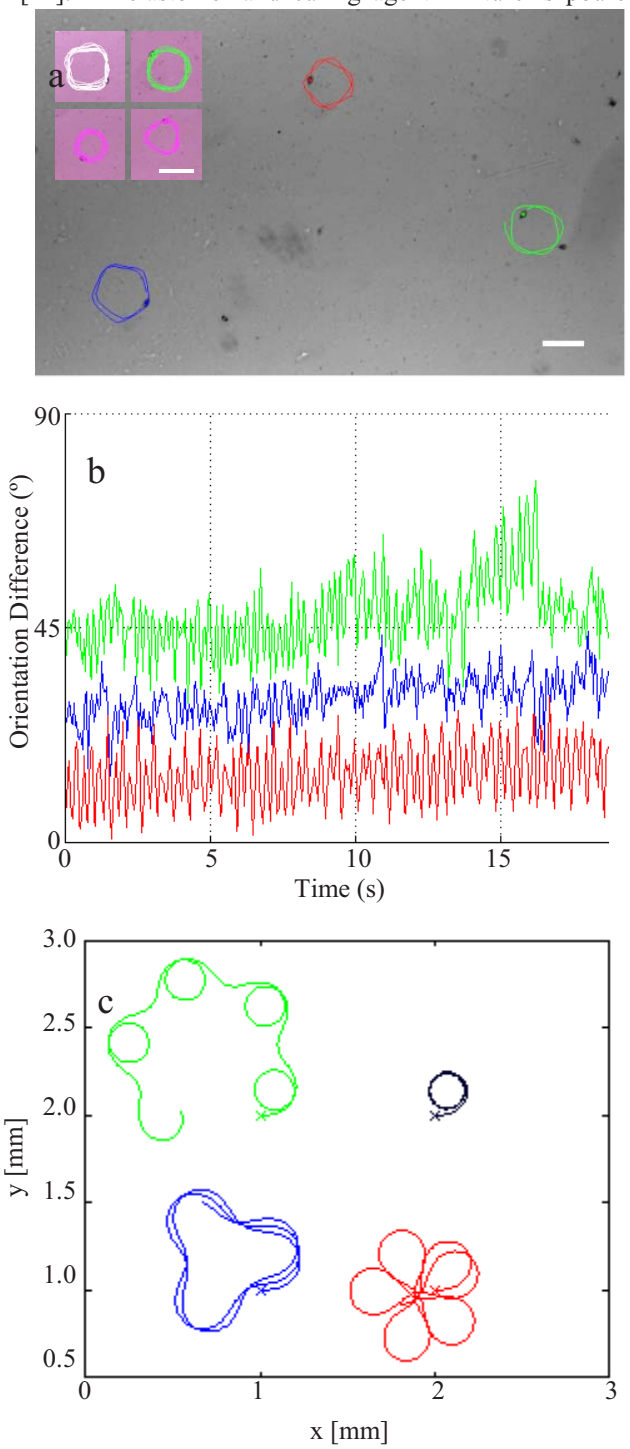

Fig. 3. (a) Three cells in a rotating magnetic field after 5 minutes. (inset) Trajectory of red cell, clockwise from top left, at t = 1 min, 5 min, 10 min, and 10 min. (b) The difference between the magnetic field orientation and the cell orientation is plotted here. The colors correspond to the top figure. (c) Four cells with different time constants simulated for ten seconds in a rotating magnetic field 6 rad/s. The black cell indicates a cell that is highly responsive to a rotating magnetic field; the others have a lower response. The scale bars are 250 µm.

3. Results and Discussion

3.1 Constantly Rotating Magnetic Fields

Cells are steered using magnetic fields. AMT are in a rotating magnetic field of 6 rad/s, seen in Fig. 3 (a). The difference between the magnetic field orientation and the cell's orientation are plotted in Fig. 3 (b). Without a magnetic field, the initial swimming trajectories of cells are random. Under these rotating magnetic fields, the cell trajectories are circular for low rotation speeds and complicated, perhaps hypotrochoidal, spiral patterns at high rotation speeds. Cells here were exposed to rotating magnetic fields for 5 minutes. There is a consistent difference between a cell's orientation and the orientation of the magnetic field. The mean difference is 20.6°, 36.6°, and 53.9° for the cells represented by the red, blue, and green plots, respectively.

The orientation difference observed here may be attributed to several factors. As *T. pyriformis* are biological organisms, there will be some variation between each cell, whether it is their speed, frequency of oscillation due to corkscrew motion, or size. Each cell also has a dipole strength which is a function of the magnetization of the particles as well as the amount of internalized magnetite. An AMT with a greater dipole strength or large amount of magnetized magnetite will show a more robust response to an applied magnetic field, aligning itself to the magnetic field faster than other AMT that may not have as high or as much dipole strength or internalized magnetite, respectively. Regardless, we see that the cell's still manages to rotate with the same frequency as the rotating magnetic field.

There is also a slight upwards trend in the orientation difference between all the cells. This trend is not

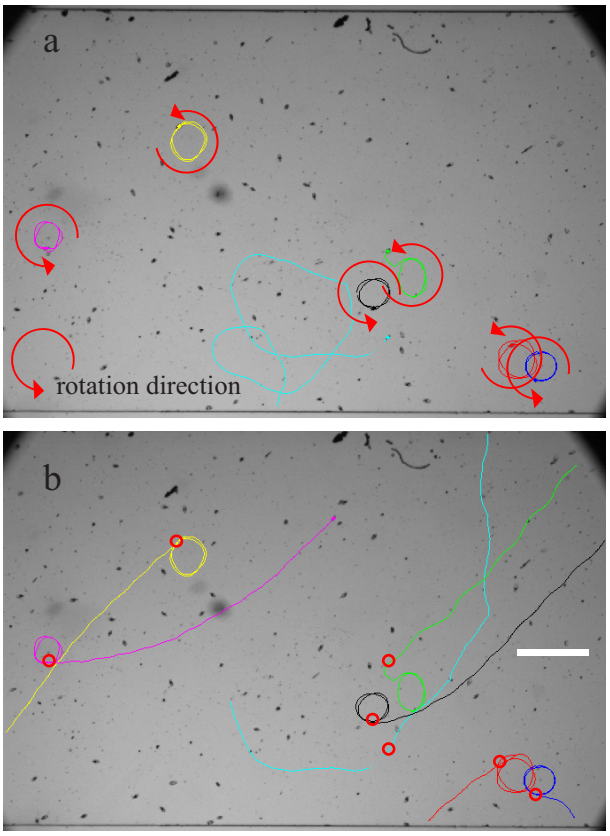

Fig. 4. (a) Trajectory of cells swimming under a 6rad/s rotating magnetic field. (b) The same cells swimming in a straight direction after the rotating magnetic field is removed. Red circles indicate the last position of the cell prior to removing the magnetic field. The scale bar is 500 μm.

consistent for these cells, as they have been swimming prior to this data capture for five minutes while matching the number of rotations and continue to do so for a remainder of 5 minutes. It is notable, however, that the cells trajectory and orientation difference will change over time. In Fig. 3 (a, inset), the trajectories of a cell when exposed to magnetic fields (6 rad/s) for 1, 5, and 10 minutes is shown. The cell also decreased speed, evident from the decrease in radius. This decrease in speed may have resulted from the cell tiring or the slight increase in temperature of the test chamber due to constant electromagnet utilization.

3.2 Removal of Magnetic Fields

Cells were placed in rotating magnetic fields (6 rad/s) for less than 10 seconds. Afterwards, the magnetic field was switched off, and the swimming of the previously rotating cells observed. Fig. 4 (a) shows cells swimming in circular trajectories while the magnetic field is on and Fig. 4 (b) shows cells after the field has been switched off. Circular trajectories varying in shape are observed for six different cells. In Fig. 5 (a), the black dashed line in the plot represents the orientation of the field. Similar to the previous experiment of extended exposure to magnetic fields, there is a slight lag between the cell's orientation

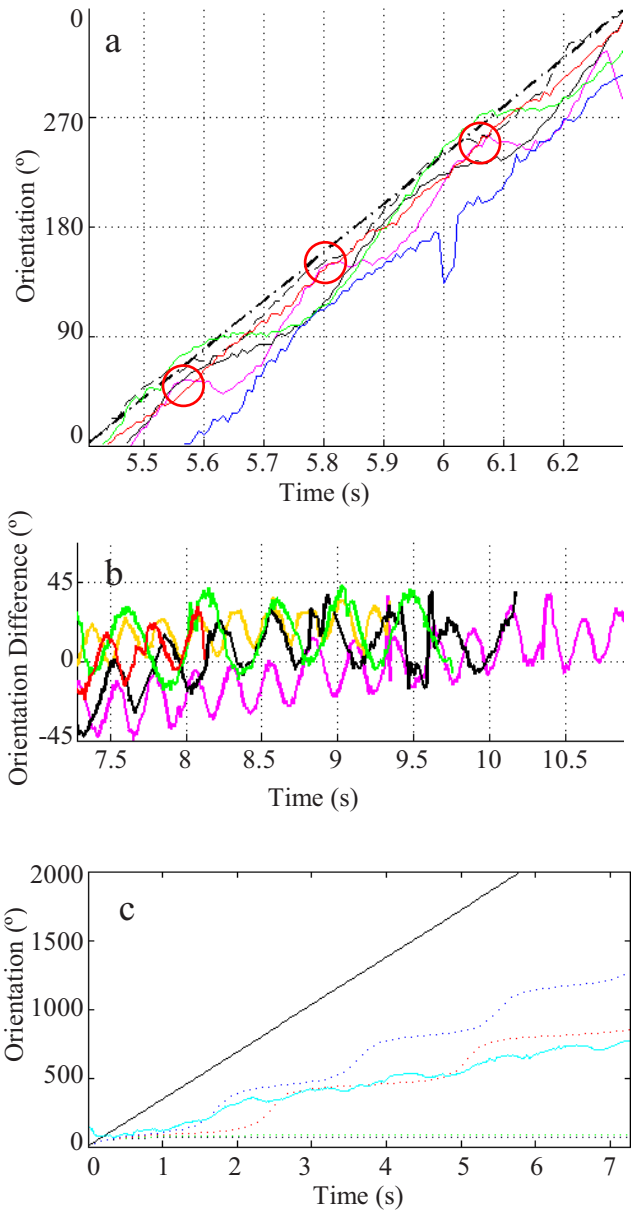

Fig. 5. (a) Cell orientation in a one period. The dashed line is the orientation of the magnetic field. Cells follow the magnetic field closely. The colors here match the cells in Fig. 4 except for the dashed black line(represented by yellow trajectory). Red circles represent kinks attributed to the cell's corkscrew motion. (b) The difference between the cell's orientation and the orientation of the magnetic field just prior to removal. Cells swim in relatively straight trajectories after removal of the magnetic field. (c) Cell with a high latency. Cells match simulation of cells that poorly follow the magnetic field.

and direction of the magnetic field. The magnetic field is removed at 7.28 seconds, during which the orientation of the field is 31.3°. At this point, the power supplies are turned off and no magnetic fields are present. The cells demonstrate typical corkscrew motion along a straight line. For 5 observed cells, the average difference between their

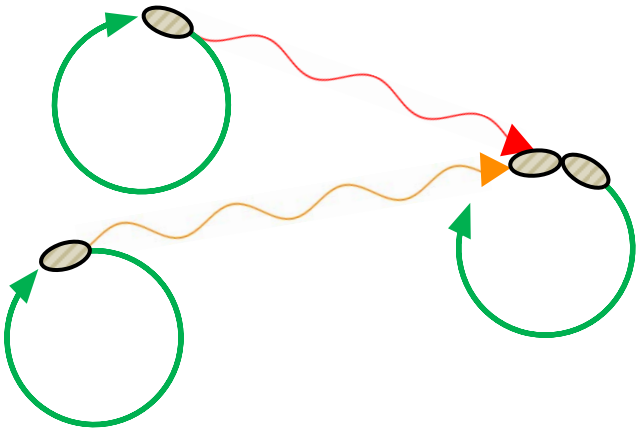

Fig. 6. A scenario for swarm control using a combination of straight and rotating swimming to direct two cells to the same orbit using a global input.

orientation and the magnetic field was 11.6°, 46.3°, 46.6°, 25.63°, and 33.8° for the cells indicated by the red, blue, yellow, magenta, and black plots, respectively. When the field was removed, however, all demonstrated straight swimming, relative to their trajectory during rotation.

During the experiment, at times a cell would overlap other cells and our image processing was unable to identify each cell. As a result, there are some brief periods where a cell could not be tracked. Outlying data points in Fig. 5, such as the blue cell at 6 sec, may be attributed to errors during centroid orientation calculations when another cell comes in close proximity or the cell swims over a distorted area (due to floating debris or interference in imaging).

In Fig. 5 (a), the cell orientations increase steadily with the magnetic fields, but there are periodic changes in slope possibly due to the cell's corkscrew swimming motion. The "kinks" for the blue, dashed black/yellow, magenta, and solid black cells during rotation are 2.0 Hz, 4.3 Hz, 4.2 Hz, and 2.4 Hz, respectively. The values for blue, dashed black/yellow, magenta, and solid black cells after the magnetic field is turned off are 2.1 Hz, 4.1 Hz, 3.8 Hz, and 2.7 Hz, respectively. The kinks for one cell are indicated by red circles in Fig. 5 (a).

Although most cells matched the rotation frequency of the magnetic field, there was one observed case where a cell could not match the frequency yet still exhibited a distinct influenced trajectory. Figure 5 (c) shows a cyan cell which follows the magnetic field periodically. As previously mentioned, *T. pyriformis* exhibit a corkscrew motion when swimming due to the angled array of cilia along the length of the cell body. The cell appeared to rotate with the field when the direction of change and orientation of the cells oscillation was similar to that of the rotating magnetic field. During this point, it is likely that the cell experiences the least amount of resistance to the magnetic field. This cell's magnetic moment may not have been as high as the other cells, resulting in the unique trajectory. The cell is plotted against a simulation (dashed lines) for cells with various time constants for aligning themselves to the magnetic field. This cell closely follows with simulated cells that exhibit poor response to magnetic fields, indicating the accuracy and potential of our model for swarm control.

3.3 Swarm Control

Once a rotating magnetic field has been removed, cells continue to swim straight, although in slightly different directions. This difference in orientation may be used to control swarms of cells to congregate or steer them to arbitrary positions. Using a combination of rotating and straight swimming (swimming in the presence and absensce of a rotating magnetic field), a scenario such as that illustrated in Fig. 7 may be accomplished with many cells. A system can implement a toggling magnetic field to characterize cells and then calculate the most efficient path for goals.

4. Conclusion

In this paper, we have characterized the swarming motion of artificially magnetotactic *T. pyriformis* in the presence and removal of rotating magnetic fields. Each cell's unique magnetic moment and other innate differences result in a lag when following a magnetic field. In a constant field, cells demonstrated a relatively even lag behind the applied fields. One case where a cell could not follow the period of the applied field still behaved predictably, verified by a simulation model of the cell. The phase lag in can also be seen when the magnetic fields are removed: cells swim straight but in various orientations. By exploiting this rotating and straight swimming, a swarm control method using rotating fields may be implemented to control a swarm of cells. Discrete control of multiple cells will enable us to perform complex microassembly and micromanipulation tasks.

Acknowledgement

This work was supported by the National Science Foundation under CMMI 1000255, CMMI 1000284, and by ARO W911F-11-1-0490.

References

[1] A. Ghosh and P. Fischer, "Controlled propulsion of artificial magnetic nanostructured propellers," *Nano letters,* vol. 9, pp. 2243-5, 2009.

[2] L. Zhang, J. J. Abbott, L. Dong, B. E. Kratochvil, D. Bell, and B. J. Nelson, "Artificial bacterial flagella: Fabrication and magnetic control," *Applied Physics Letters,* vol. 94, pp. 064107-064107, 2009.

[3] K. E. Peyer, S. Tottori, F. Qiu, L. Zhang, and B. J. Nelson, "Magnetic Helical Micromachines," *Chemistry (Weinheim an der Bergstrasse, Germany),* pp. 28-38, 2012.

[4] K. E. Peyer, L. Zhang, and B. J. Nelson, "Bio-inspired magnetic swimming microrobots for biomedical applications," *Nanoscale,* 2012.

[5] S. Tottori, L. Zhang, F. Qiu, K. K. Krawczyk, A. Franco-Obregón, and B. J. Nelson, "Magnetic

helical micromachines: fabrication, controlled swimming, and cargo transport," *Advanced materials (Deerfield Beach, Fla.),* vol. 24, pp. 811-6, 2012.

[6] L. Zhang, K. E. Peyer, and B. J. Nelson, "Artificial bacterial flagella for micromanipulation," *Lab on a Chip,* vol. 10, pp. 2203-2215, 2010.

[7] R. Dreyfus, J. Baudry, M. L. Roper, M. Fermigier, H. A. Stone, and J. Bibette, "Microscopic artificial swimmers," *Nature,* vol. 437, pp. 862-865, 2005.

[8] L. Zhang, T. Petit, K. E. Peyer, and B. J. Nelson, "Targeted cargo delivery using a rotating nickel nanowire," *Nanomedicine: Nanotechnology, Biology and Medicine,* vol. 8, pp. 1074-1080, 2012.

[9] D. B. Weibel, P. Garstecki, D. Ryan, W. R. DiLuzio, M. Mayer, J. E. Seto*, et al.*, "Microoxen: microorganisms to move microscale loads," *Proceedings of the National Academy of Sciences of the United States of America,* vol. 102, pp. 11963-7, 2005.

[10] U. K. Cheang, D. Roy, J. H. Lee, and M. J. Kim, "Fabrication and magnetic control of bacteria-inspired robotic microswimmers," *Applied Physics Letters,* vol. 97, pp. 213704-213704-3, 2010.

[11] M. Kim, E. Steager, A. A. Julius, and J. Agung, *Microbiorobotics: biologically inspired microscale robotic systems*: William Andrew, 2012.

[12] N. Ogawa, H. Oku, K. Hashimoto, and M. Ishikawa, "A physical model for galvanotaxis of Paramecium cell," *Journal of theoretical biology,* vol. 242, pp. 314-28, 2006.

[13] I. D. Brown, J. G. Connolly, and G. Kerkut, "Galvanotaxic response of Tetrahymena vorax," *Comparative Biochemistry and Physiology Part C: Comparative Pharmacology,* vol. 69, pp. 281-291, 1981.

[14] D. H. Kim, D. Casale, L. Köhidai, and M. J. Kim, "Galvanotactic and phototactic control of Tetrahymena pyriformis as a microfluidic workhorse," *Applied Physics Letters,* vol. 94, pp. 163901-163901, 2009.

[15] L. Köhidai and G. Csaba, "Chemotaxis and chemotactic selection induced with cytokines (IL-8, Rantes and TNF-α) in the unicellular Tetrahymena pyriformis," *Cytokine,* vol. 10, pp. 481-486, 1998.

[16] S.-W. Nam, D. Van Noort, Y. Yang, and S. Park, "A biological sensor platform using a pneumatic-valve controlled microfluidic device containing Tetrahymena pyriformis," *Lab on a chip,* vol. 7, pp. 638-40, 2007.

[17] S. Martel, O. Felfoul, J.-B. Mathieu, A. Chanu, S. Tamaz, M. Mohammadi*, et al.*, "MRI-based Medical Nanorobotic Platform for the Control of Magnetic Nanoparticles and Flagellated Bacteria for Target Interventions in Human Capillaries," *The International journal of robotics research,* vol. 28, pp. 1169-1182, 2009.

[18] S. Martel, M. Mohammadi, O. Felfoul, Z. Lu, and P. Pouponneau, "Flagellated Magnetotactic Bacteria as Controlled MRI-trackable Propulsion and Steering Systems for Medical Nanorobots Operating in the Human Microvasculature," *The International journal of robotics research,* vol. 28, pp. 571-582, 2009.

[19] S. Martel, C. C. Tremblay, S. Ngakeng, and G. Langlois, "Controlled manipulation and actuation of micro-objects with magnetotactic bacteria," *Applied Physics Letters,* vol. 89, pp. 233904-233904, 2006.

[20] D. H. Kim, P. S. S. Kim, A. A. Agung Julius, and M. J. Kim, "Three-dimensional control of Tetrahymena pyriformis using artificial magnetotaxis," *Applied Physics Letters,* vol. 100, pp. 053702-053702-3, 2012.

[21] Y. Ou, D. H. Kim, P. Kim, M. J. Kim, and A. A. Julius, "Motion control of magnetized Tetrahymena pyriformis cells by magnetic field with Model Predictive Control," *The International Journal of Robotics Research,* 2012.

[22] D. H. Kim, S. Brigandi, A. A. Julius, and M. J. Kim, "Real-time feedback control using artificial magnetotaxis with rapidly-exploring random tree (RRT) for Tetrahymena pyriformis as a microbiorobot," *2011 IEEE International Conference on Robotics and Automation,* pp. 3183-3188, 2011.

[23] L. Köhidai and G. Csaba, "Effects of the mammalian vasoconstrictor the immunocytological detection of endogenous activity," *Comparative Biochemistry and Physiology Part C: Pharmacology, Toxicology and Endocrinology,* vol. 111, pp. 311-316, 1995.

[24] B. H. Jo, L. M. Van Lerberghe, K. M. Motsegood, and D. J. Beebe, "Three-dimensional micro-channel fabrication in polydimethylsiloxane (PDMS) elastomer," *Microelectromechanical Systems, Journal of,* vol. 9, pp. 76-81, 2000.